



**INSTITUTE OF HIGH ENERGY PHYSICS
CHINESE ACADEMY OF SCIENCES**

All-fiber optical-microwave phase detector for laser-RF synchronization

Hao Zeng, Jingyi Li, Xinpeng Ma, Nan Gan

Institute of High Energy Physics
Chinese Academy of Sciences

30/10/2024



Outline

- Background
- Proposal Design
 - All-fiber optical-microwave phase detector (AFOM-PD)
 - Femtosecond synchronization system based on AFOM-PDs
- Experimental Results
- Future plans

Background

- Precise and stable synchronization between a mode-locked laser and a microwave oscillator is crucial for fields like telecommunications, radio astronomy and metrology;
- Especially, the ultrafast electron diffraction (*UED*) facilities and the X-ray free-electron laser (*XFEL*) are prime examples of femtosecond-level, high-precision laser-microwave synchronization systems applied in accelerators.

Background

- RF accelerator-based *UED facilities* and *XFELs* :
 - ❑ Probes: *ultrashort electron pulses* and *X – ray pulses*;
 - ❑ Synchronization precision: at least comparable to pulse width, typically ~ 10 fs or even \sim fs level.
- Photocathode injectors and RF acceleration structures in *UED facilities* and *XFELs*:
 - ❑ Electron bunches in stable RF acceleration phase for optimal acceleration efficiency.

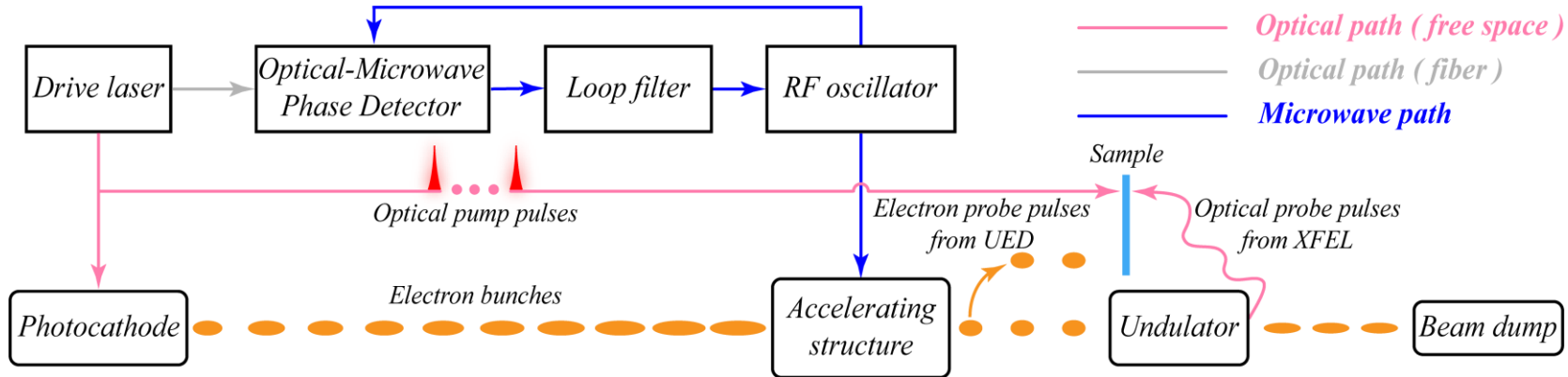


Fig.1 Schematic of optical-microwave synchronization system based on optoelectronic phase-locked loop



Beam-Driven PWFA in IHEP

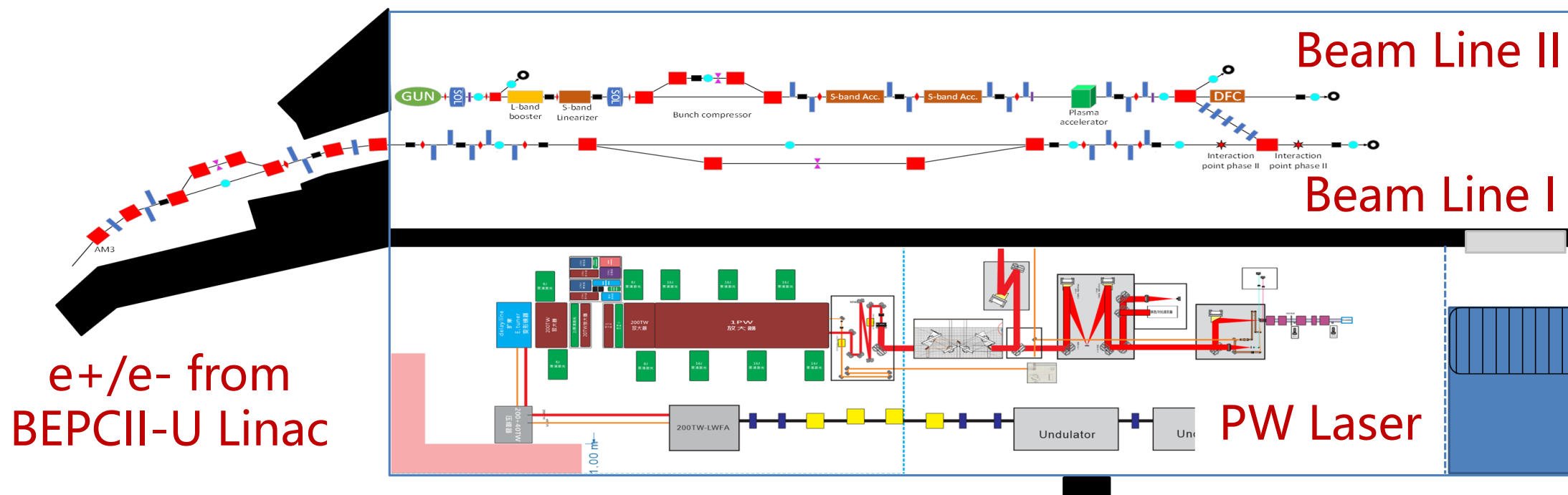


Fig.2 Beam-driven PWFA in IHEP

- Demo.1: PWFA in new photon-cathode 150 MeV Linac by two-bunch train.
- Demo.2: Positron bunch from BEPCII-U Linac is driven by electron bunch of new Linac.
- Demo.3: First cascaded PWFA by accelerated electron bunch together with e+/e- from BEPCII-U Linac.
- Demo.4: PetaWatts laser can be used in laser-driven plasma wakefield acceleration.



Phase Reference for PWFA Linac LLRF

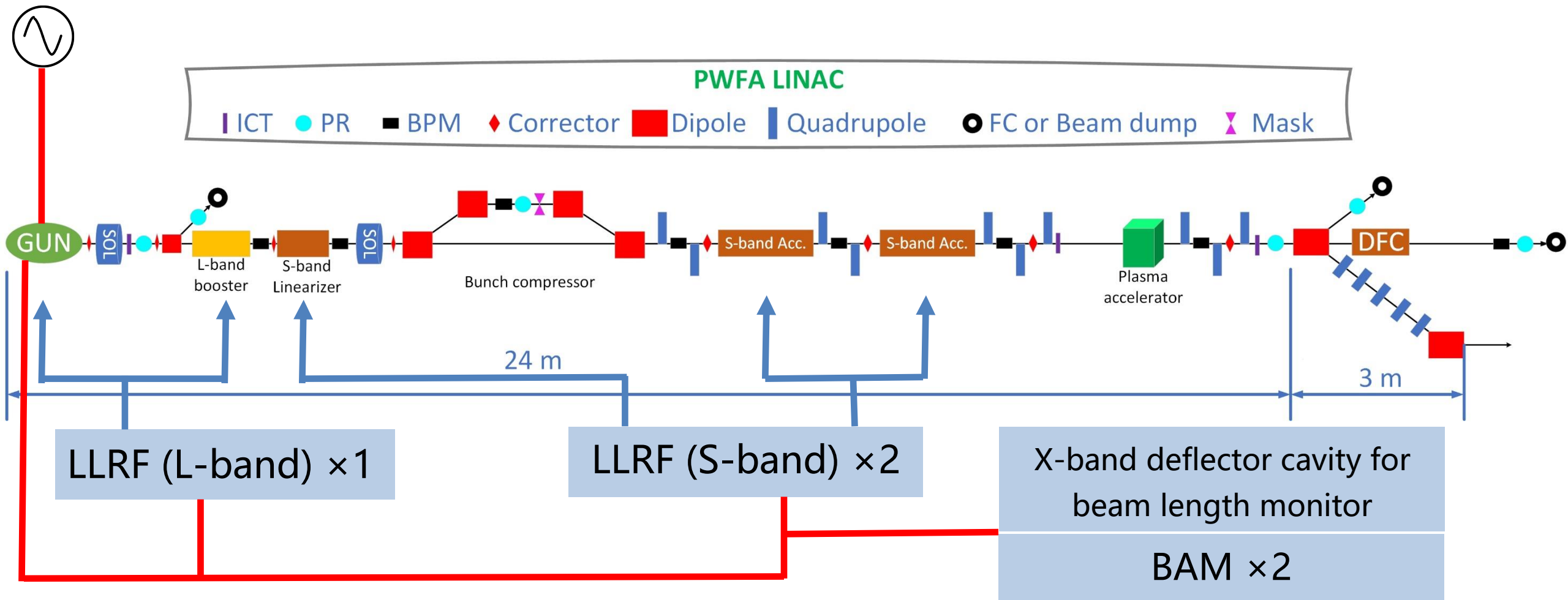


Fig.3 Phase reference for PWFA Linac LLRF

Proposal Design

- Design of optical-microwave phase detectors;
- Design of synchronization and testing system.

Synchronization System Based On AFOM-PD

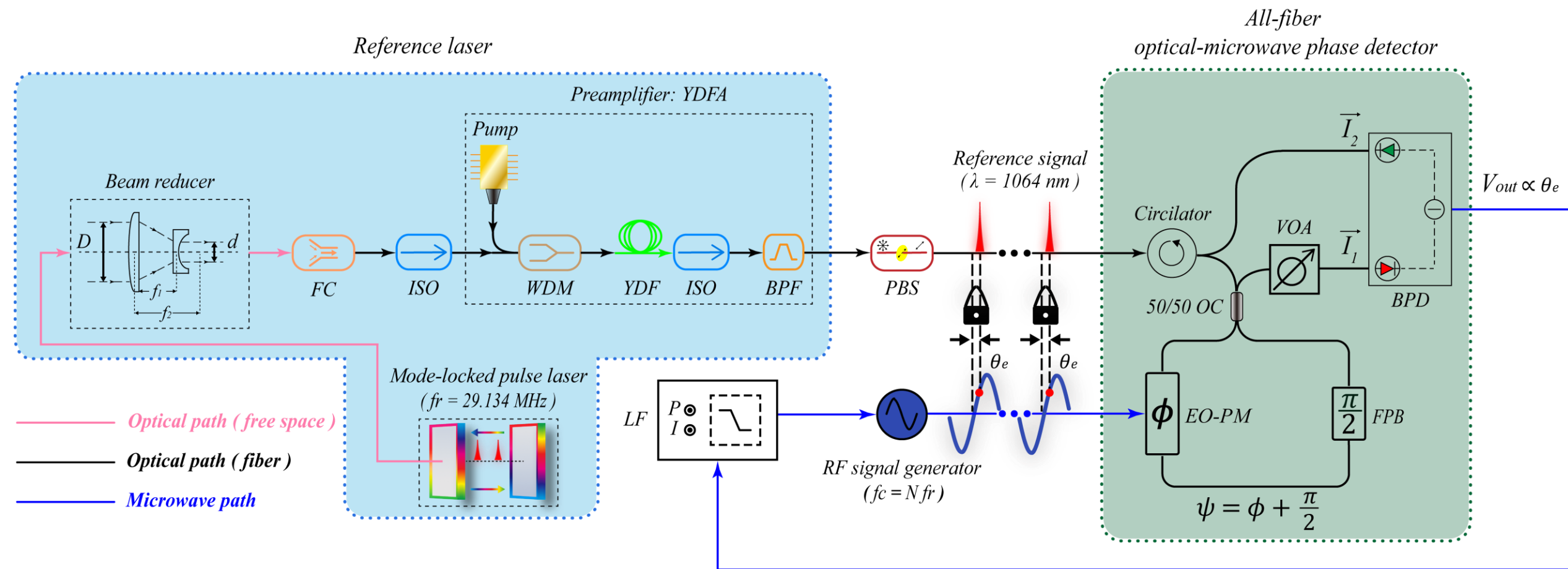


Fig.4 Laser-RF synchronization system based on AFOM-PD

Laser Beam Reducer

- Taking into the need for actual coupling efficiency, a Galilean beam reducer composed of a plano-concave lens with a focal length of -25 mm and a plano-convex lens with a focal length of 75 mm was selected, resulting in a beam reduction ratio of 3.

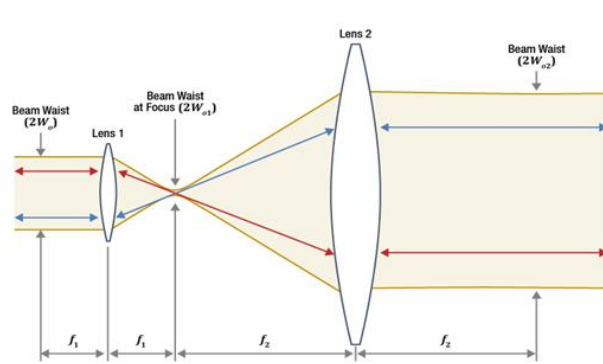


Fig.5 Keplerian beam reducer^[1]

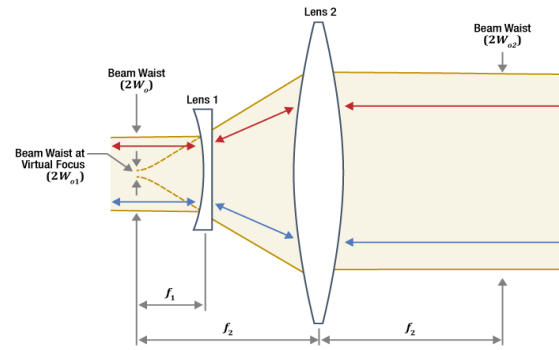


Fig.6 Galilean beam reducer^[2]

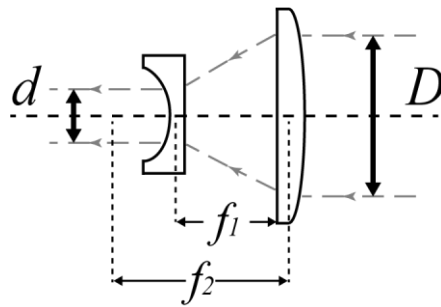


Fig.7 Galilean beam reducer used in the experiment



Fig.8 Beam reducer and collimator

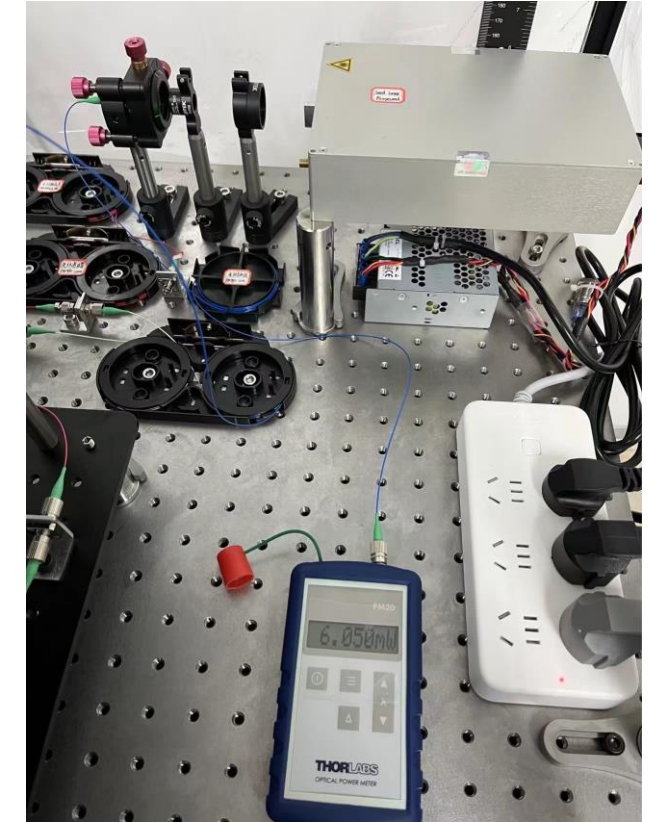


Fig.9 Seed laser coupling power is 6 mW

[1-2] Thorlabs. Does it matter whether a beam expander or reducer has a Keplerian or Galilean design?EB/OL].(2021-07-02)[2024-04-17]. https://www.thorlabs.com/newgrouppage9.cfm?objectgroup_id=14648



RIN Suppression

- Seed laser power instability:
 - ❑ Peak-to-peak $\approx 4.8\%$
 - ❑ RMS $\approx 0.5\%$
- RIN suppression
 - ❑ nonlinear amplification characteristics of a fiber amplifier in saturation.
- Fiber amplifier:
 - ❑ Pump method;
 - ❑ Pump laser wavelength;
 - ❑ Type and length of gain fiber.

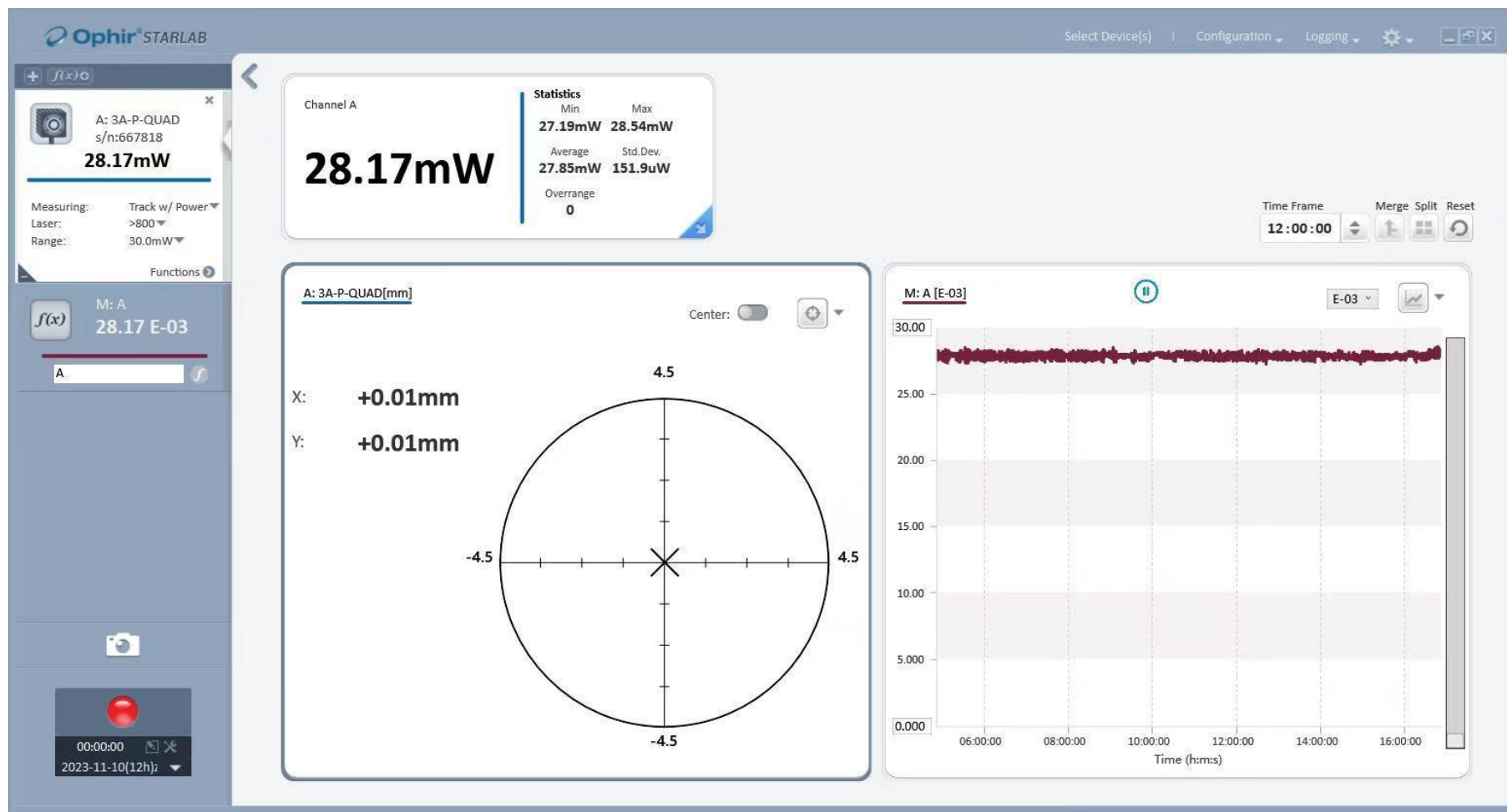


Fig.10 Measurement result of Huaray Oliver-S power stability



Yb-doped Fiber PreAmplifier (YDFA): Pumping Method

- Ytterbium-doped fiber has an emission peak at the wavelength about 1 μm ;
- Considering all factors, a co-pumping method was chosen to limit the noise figure.

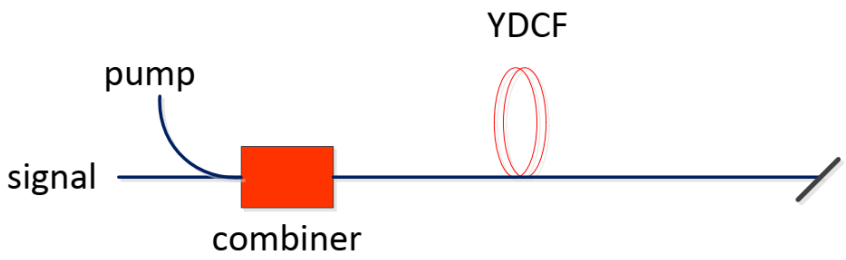


Fig.11 Co-pumping method

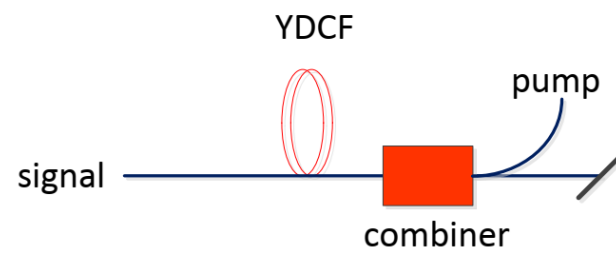


Fig.12 Counter-pumping method

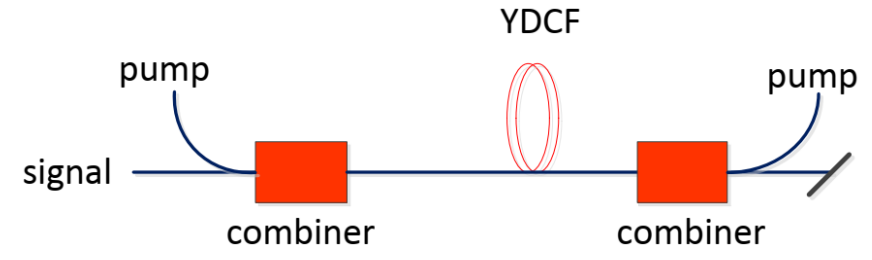


Fig.13 Bi-directional pumping method

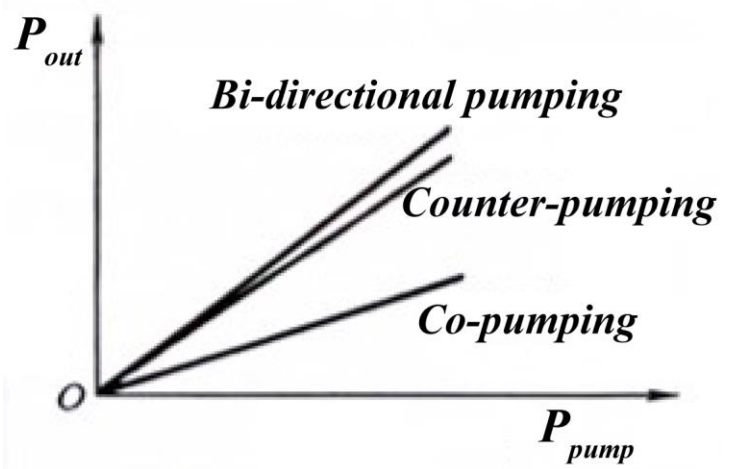


Fig.14 P_{out} VS P_{pump} [3]

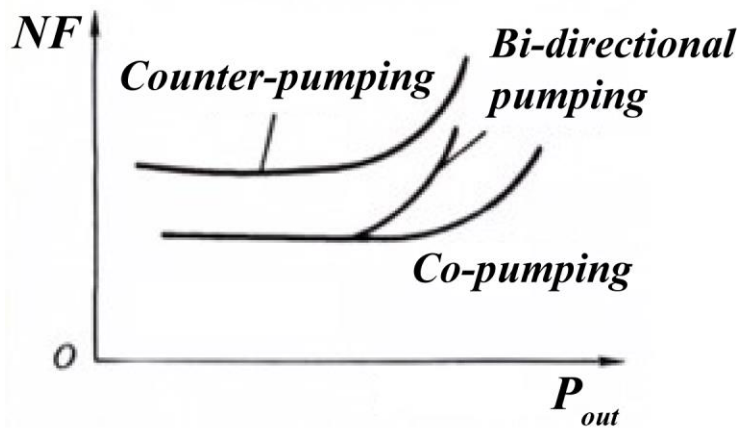


Fig.15 NF VS P_{out} [4]

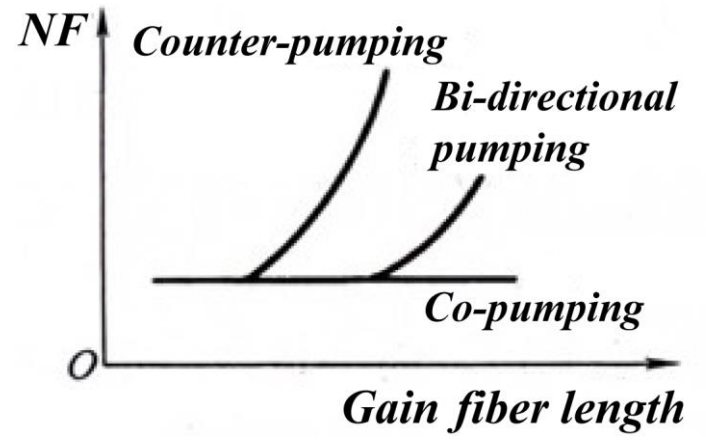


Fig.16 NF VS Gain fiber length [5]

[3-5] Shen, J., Chen, J., & Li, L. (2014). Optical Fiber Communication Systems (3rd ed.). Beijing: Mechanical Industry Press.



Yb-doped Fiber PreAmplifier (YDFA): Spectral Filtering

- Absorption peak at **975 nm**;
- For Yb-doped fiber with high doping concentration, a fiber length of about **4 m**, under a pumping power of **500 mW**, places the preamplifier output in the state of saturation;
- During ASE process, there is a higher population inversion at the wavelength of 1030 nm, which easily generates 1030 nm optical signal. To address this, a **2-nm bandwidth** bandpass filter is used to purify the spectral.

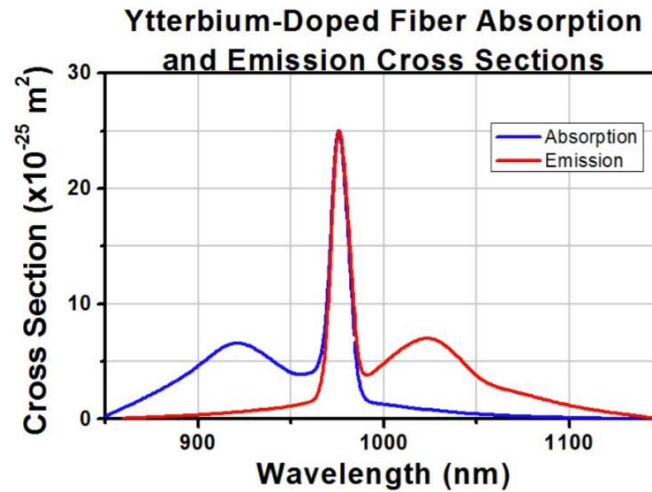


Fig.17 Absorption and emission spectra of Yb-doped fiber

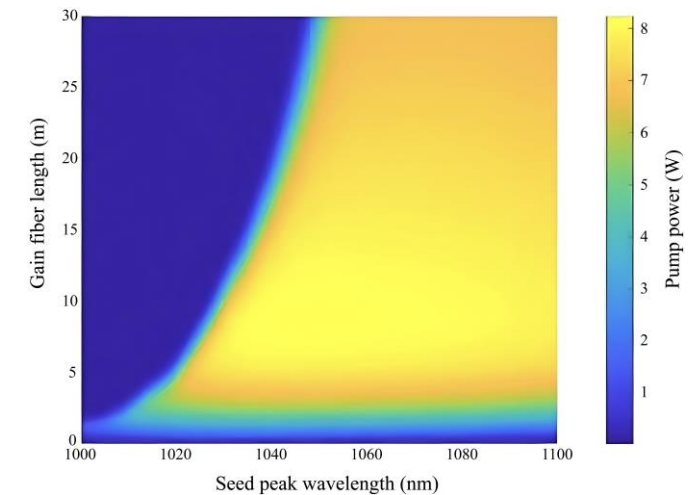


Fig.18 P_{out} VS Gain fiber length @ $P_{pump} = 500$ mW

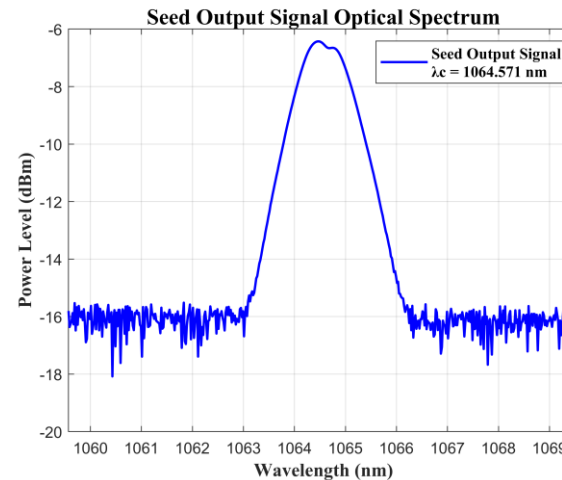


Fig.19 Spectral of 1064 nm seed laser

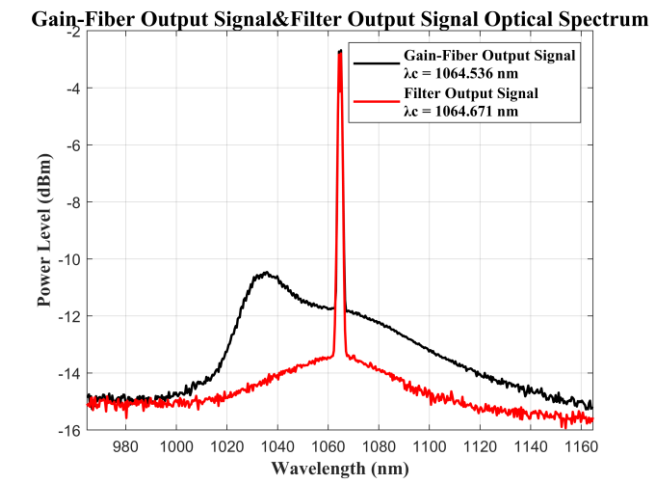


Fig.20 Spectra before & after bandpass filter



Yb-doped Fiber PreAmplifier (YDFA): RIN Suppression

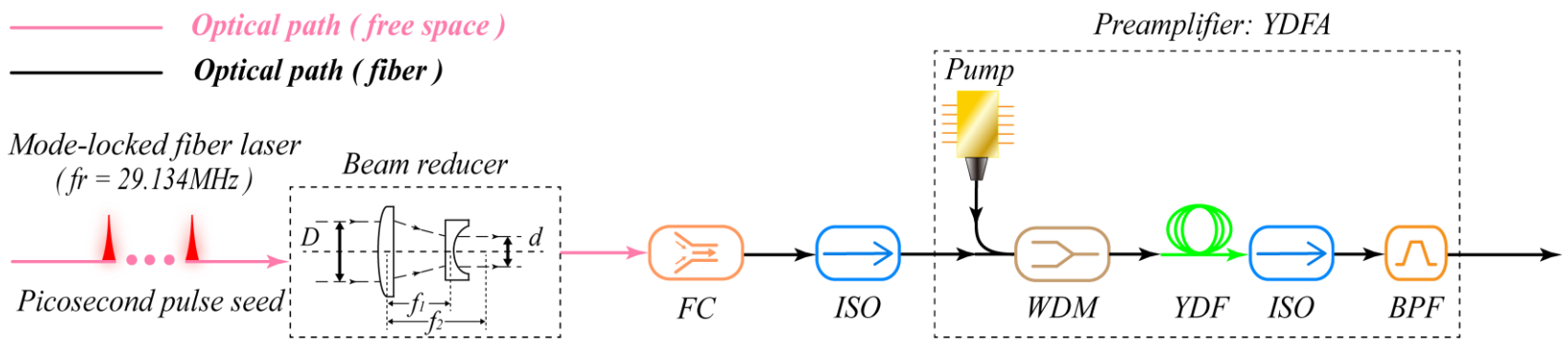


Fig.21 Laser beam reducer, collimator and YDFA

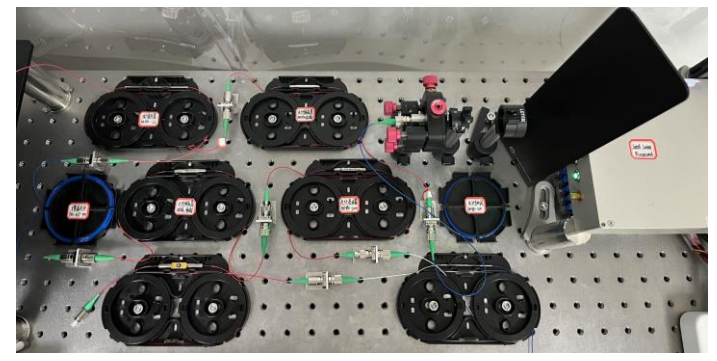


Fig.22 Reference laser

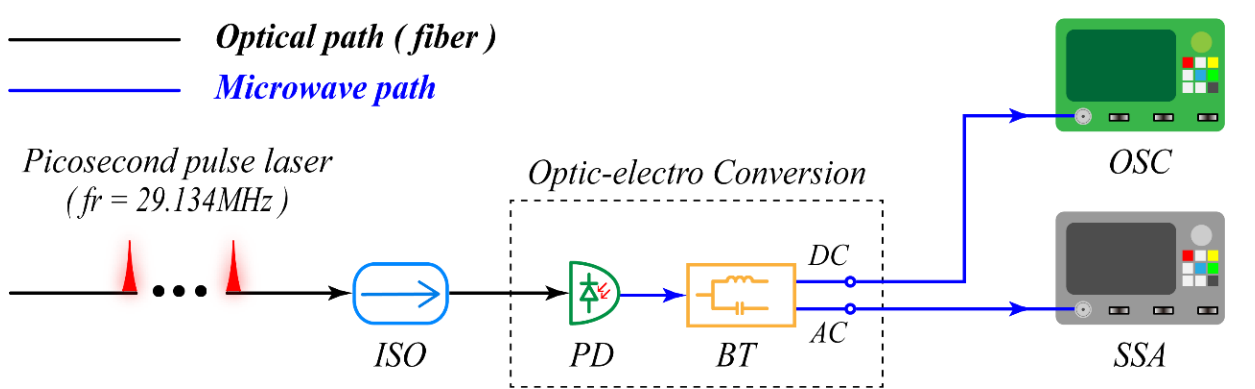


Fig.23 RIN measurement method

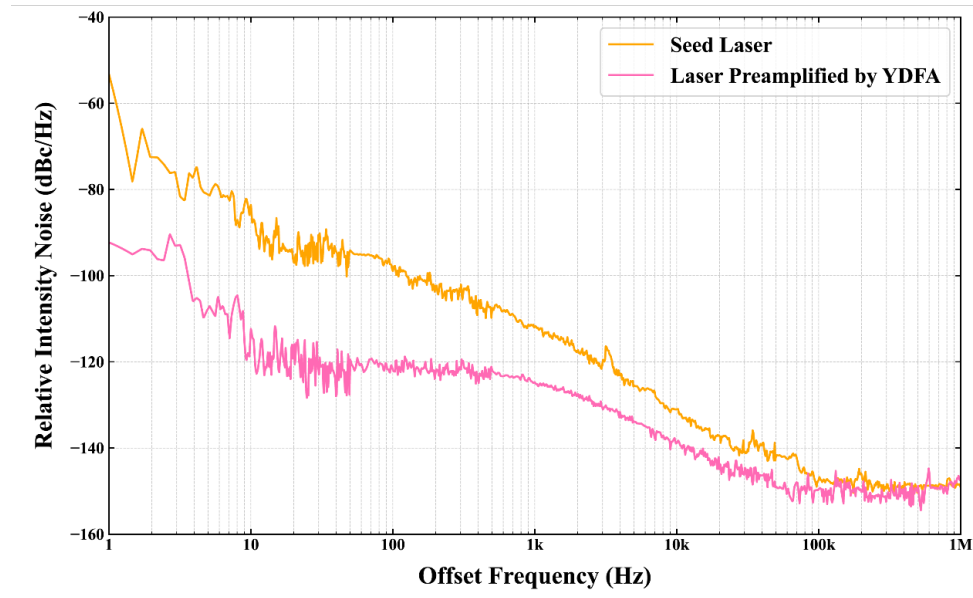


Fig.24 RIN measured before & after YDFA

AFOM-PD

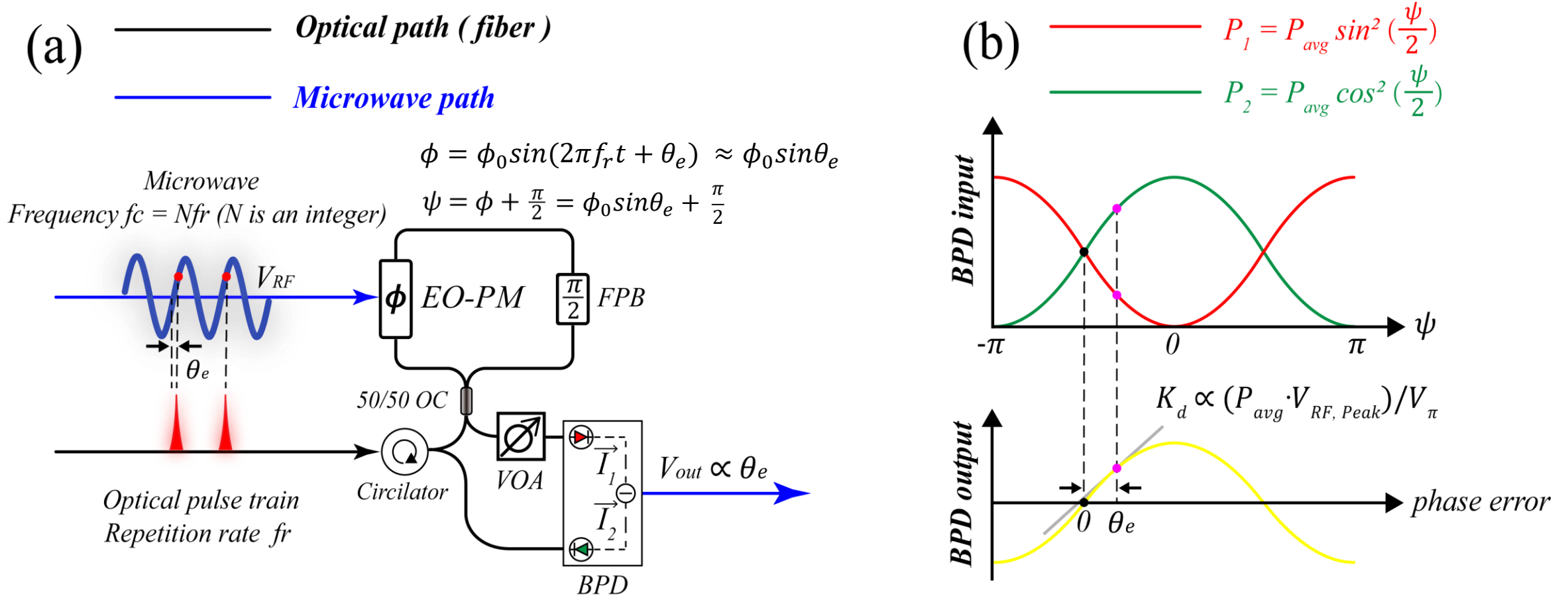


Fig.25 All-fiber optical-microwave phase detector (AFOM-PD)

(a) AFOM-PD principle;

(b) I/O characteristic curve of BPD in AFOM-PD.

Inherent phase bias: $\pi/2$

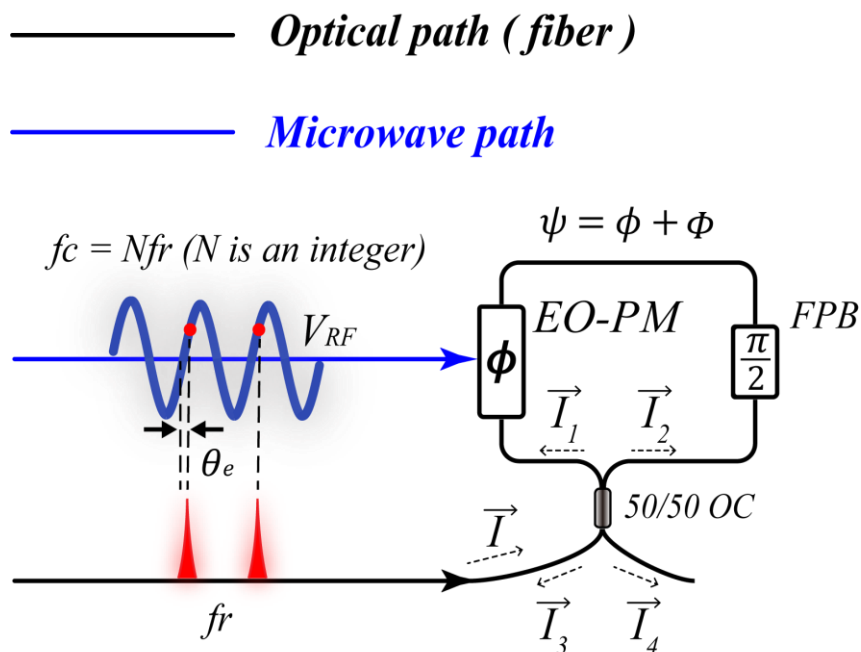


Fig.26 Sagnac fiber interference loop

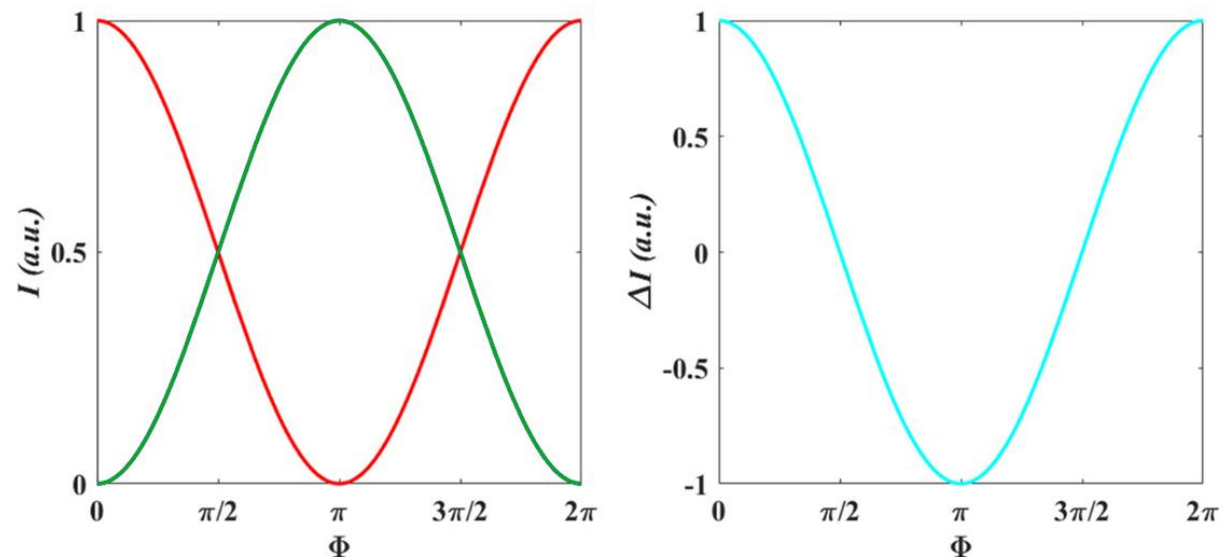


Fig.27 Intensity of the two optical output from Sagnac loop (left)

Intensity difference VS inherent bias phase (right)

- The splitting ratio of fiber coupler is 50:50. When there is no microwave modulation, the intensity of two optical output can be described as:

$$\frac{I_3}{I} = \sin^2\left(\frac{\Phi}{2}\right) = \frac{1}{2}(1 + \cos\Phi), \quad \frac{I_4}{I} = \cos^2\left(\frac{\Phi}{2}\right) = \frac{1}{2}(1 - \cos\Phi)$$



Fiber Non-reciprocal Phase Bias Unit

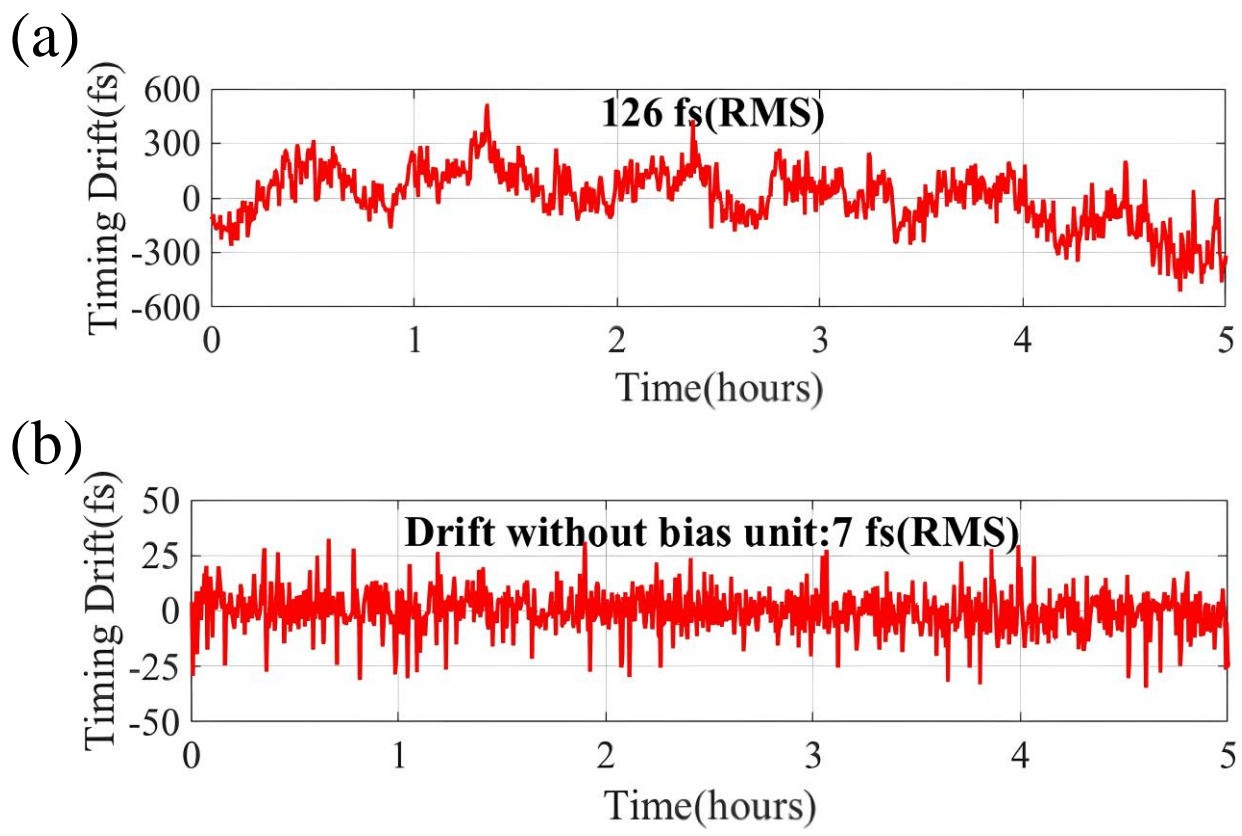


Fig.28 Measured time drift values without microwave modulation (no temperature or humidity control)
 (a) Using magneto-optical components;
 (b) Using fiber phase shifter.

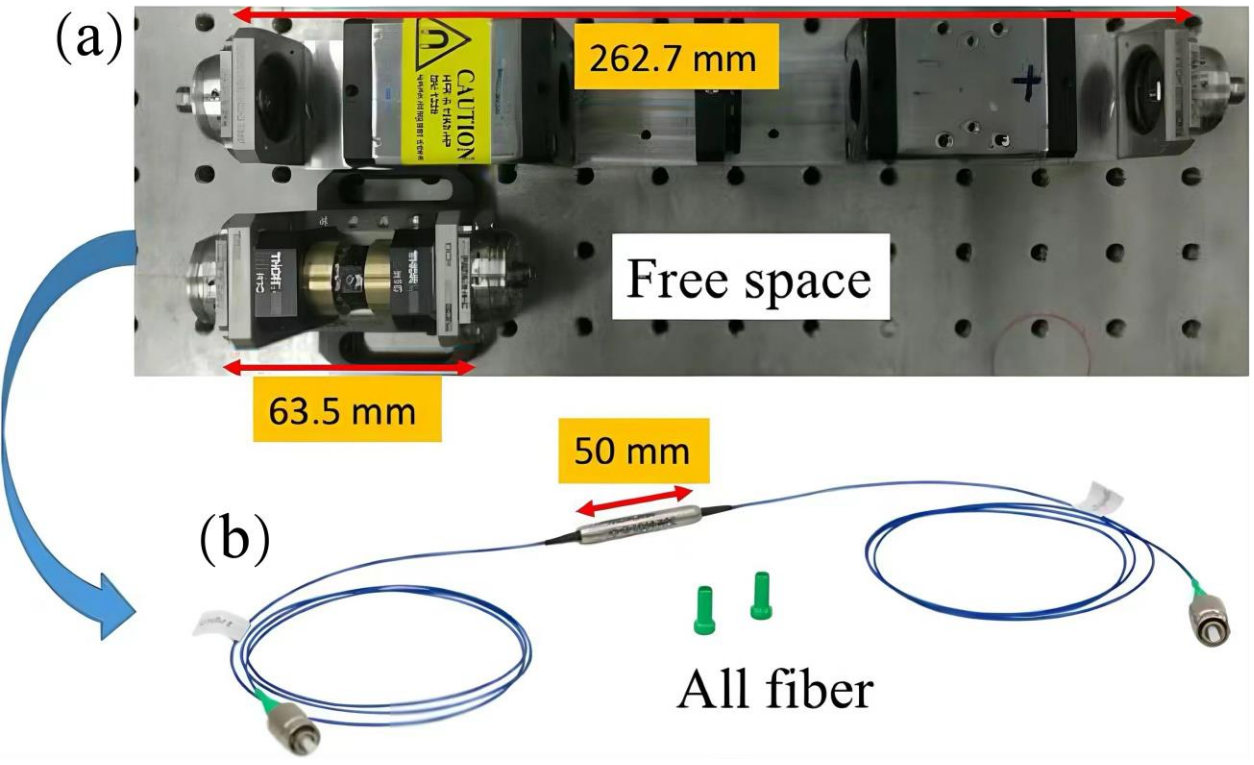


Fig.29 Non-reciprocal phase bias unit
 (a) Magneto-optical components;
 (b) Fiber phase shifter.



Microwave Voltage-controlled Oscillator

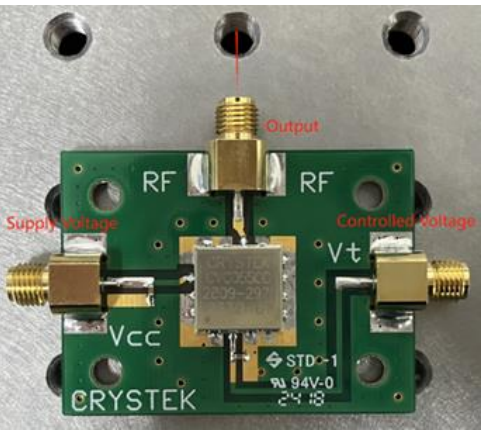


Fig.30 Crystek CVCO55CC-2809-2921 CRO

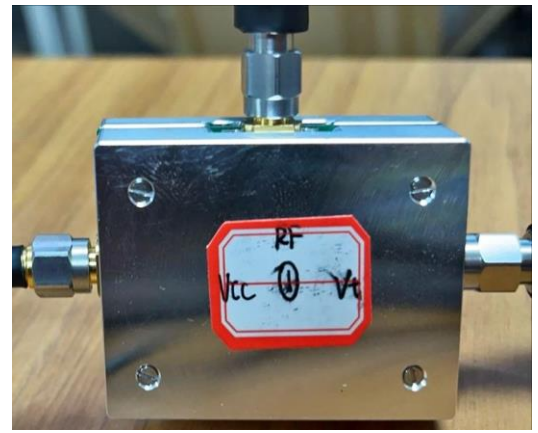


Fig.31 R&S SMA100B



Fig.32 Agilent E4428C



Fig.33 Keysight E8257D



Does Laser Pulse Width Affect Phase Detection Sensitivity?

- Simulation: for picosecond laser, under modulation depth of π , 2π , 3π , the variation in phase detection sensitivity due to pulse broadening.
 - ❑ When the microwave frequency is relatively low, the impact of laser pulse broadening on the output voltage of the phase detector can be neglected;
 - ❑ Choosing a picosecond laser as the reference laser can alleviate the impact of pulse broadening on phase detection.

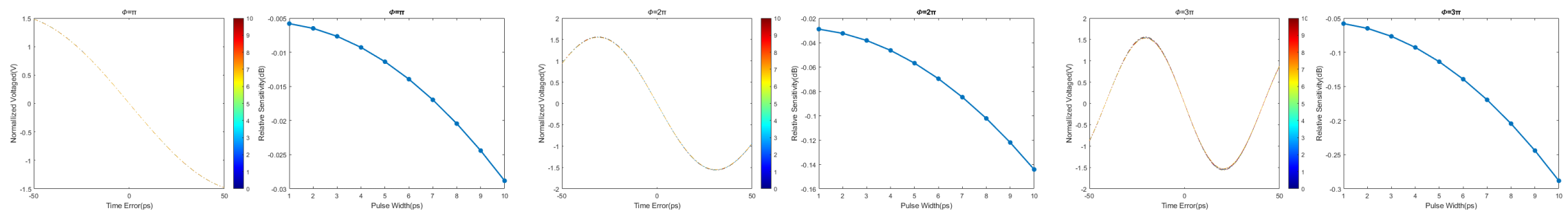


Fig.34 Output curves of AFOM-PD under 1.311030 GHz microwave modulation with pulse broadening

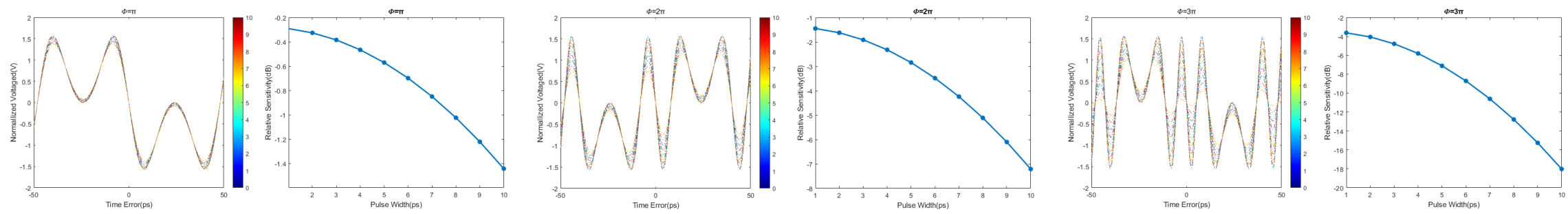


Fig.35 Output curves of AFOM-PD under 2.855132 GHz microwave modulation with pulse broadening



What Is the Appropriate Microwave Modulation Depth?

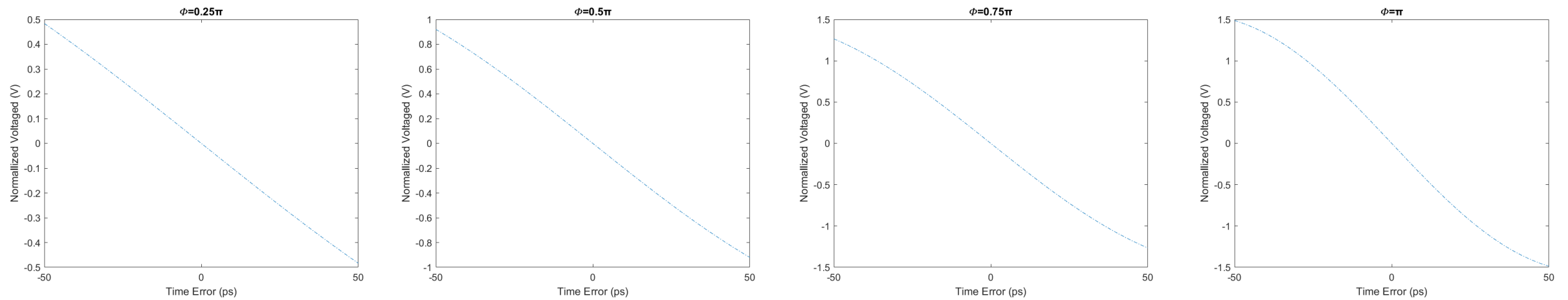


Fig.36 Output curves of AFOM-PD at 0.25π , 0.5π , 0.75π , π modulation depth of 1.311030 GHz microwave

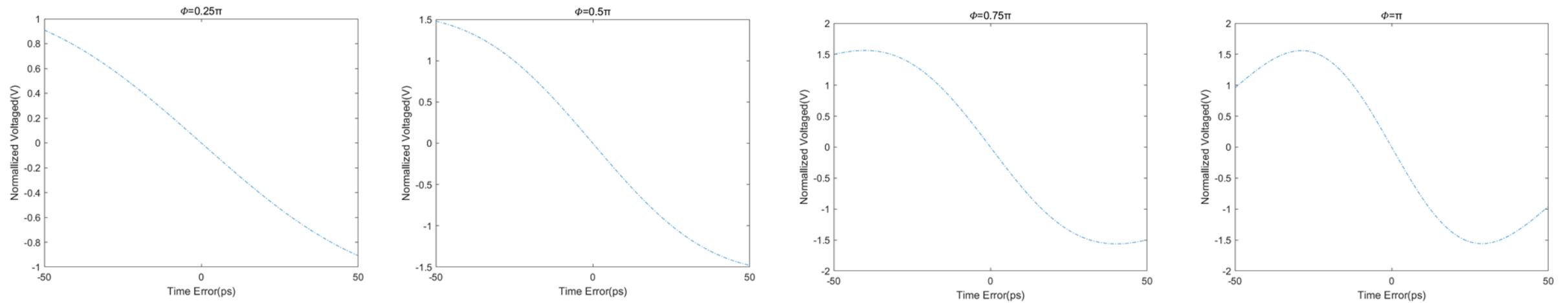


Fig.37 Output curves of AFOM-PD at 0.25π , 0.5π , 0.75π , π modulation depth of 2.855132 GHz microwave



Microwave Modulation Depth

- The modulation depth of EO-PM for the forward-propagating laser is:

$$\Phi_0 = \frac{\pi}{V_\pi} V_0$$

- Microwave power is represented by the power corresponding to the effective voltage, with a load resistance of 50 Ω for the EO-PM:

$$P_{0,RMS} = \frac{V_{0,RMS}^2}{R}$$

- The modulation depth is characterized as:

$$\Phi_0 = \frac{10\pi}{V_\pi} \sqrt{P_{0,rms}}$$

- The output power from the PSG is 24.5 dBm. After passing through the power splitter and RF cables, the input microwave power to the EO-PM is 20.8 dBm. The EO-PM has half-wave voltages of 3.8 V and 4.4 V at frequencies of 1.311010 GHz and 2.855132 GHz, corresponding to phase detector microwave modulation depths of 0.90π and 0.78π .

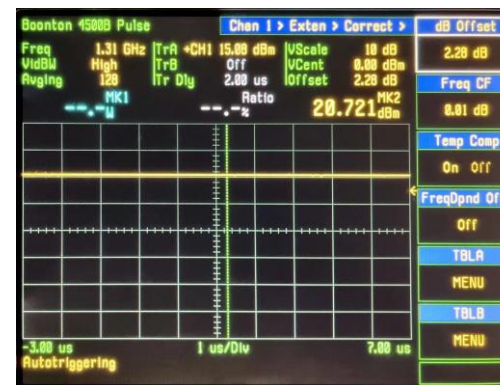


Fig.38 The measured 1.311030 GHz microwave power output from the PSG



Fig.39 The measured 2.855132 GHz microwave power output from the PSG

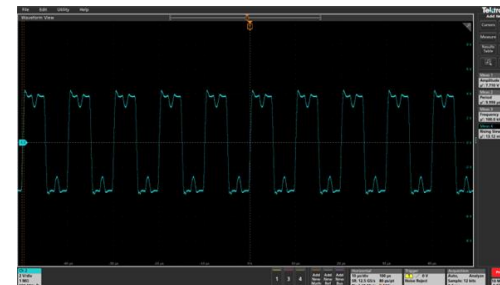


Fig.40 Error waveform at 1.311030 GHz

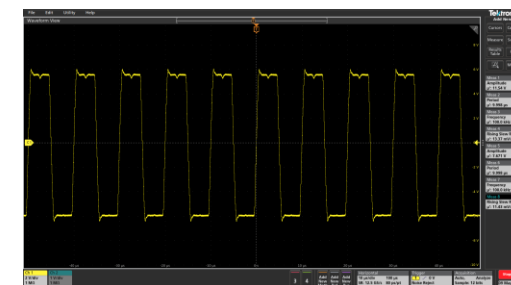


Fig.41 Error waveform at 2.855132 GHz



Experimental Setup

- Two sets of AFOM-PDs:
 - ❑ In-loop AFOM-PD: phase-locked;
 - ❑ Out-of-loop AFOM-PD: testing and analysis.
- Performance consistency:
 - ❑ Phase detection sensitivity;
 - ❑ Optical power loss.
- Synchronization and testing setup:
 - ❑ Balance the optical path difference and optical intensity difference inside and outside the loop;
 - ❑ Ensure the modulation microwave phases inside and outside the loop are the same.

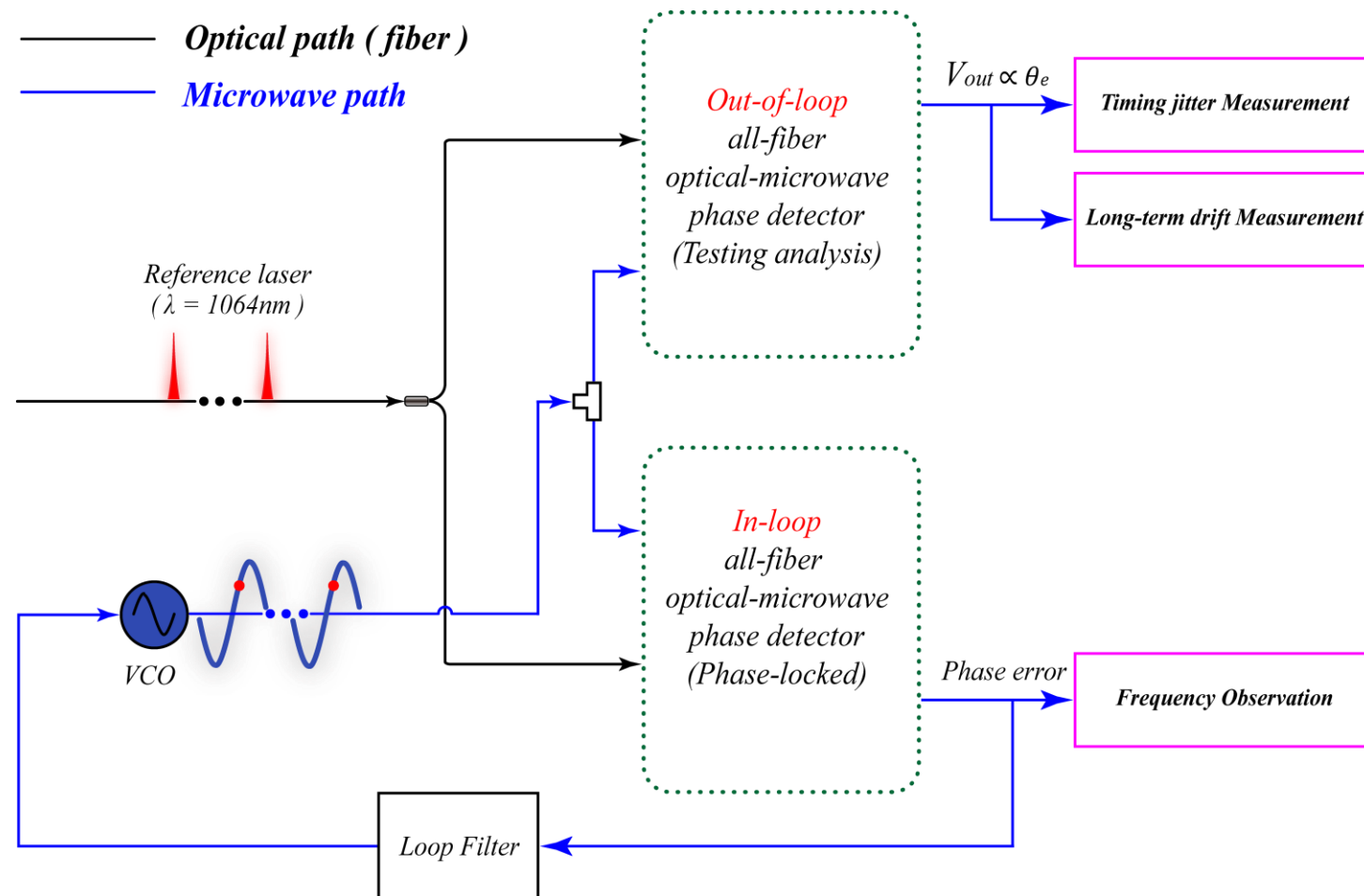


Fig.42 Synchronization and testing system setup



Optical Path and Optical Intensity Balance

➤ An adjustable phase delay line and a variable optical attenuator are used to balance in-loop and out-of-loop optical path and intensity.

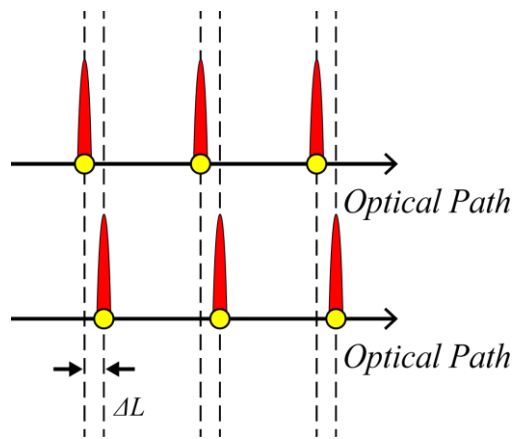


Fig.43 Optical path difference

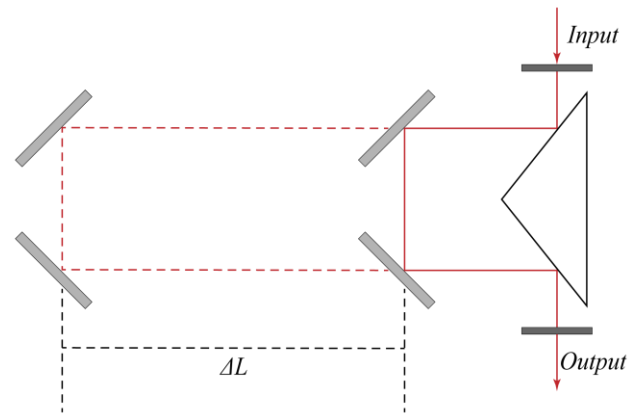


Fig.44 Schematic of adjustable phase delay line

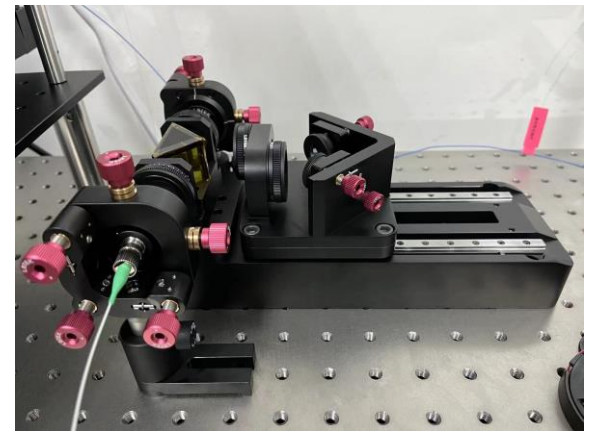


Fig.45 Adjustable phase delay line

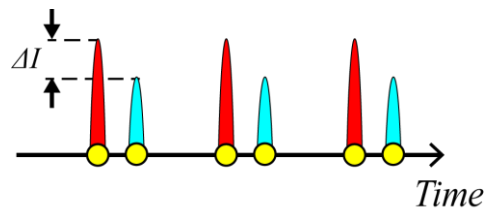


Fig.46 Optical intensity difference

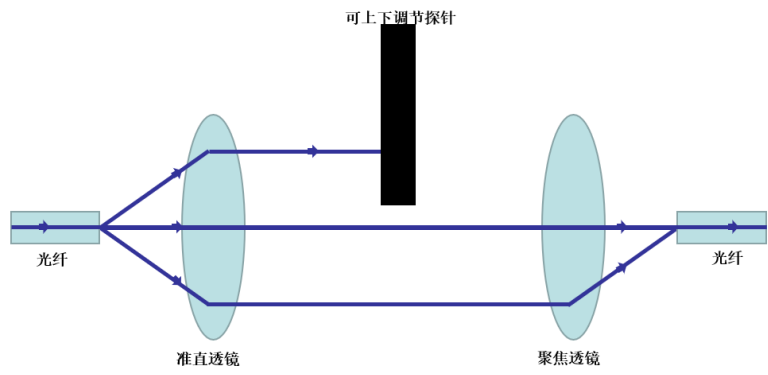


Fig.47 Schematic variable optical attenuator

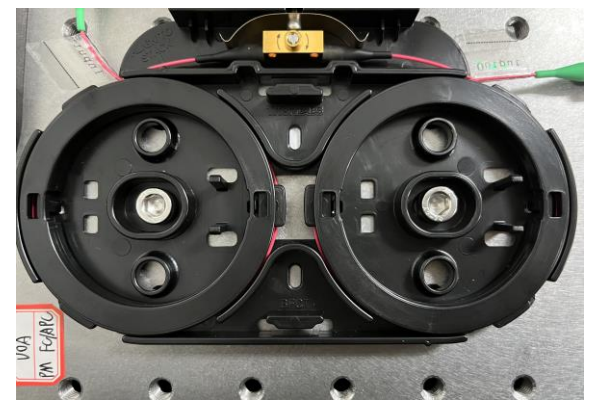


Fig.48 Variable optical attenuator

Modulation Microwave Phases Balance

- Two mechanical phase shifter (6708-2, Sage) are used to ensure the phase balance between in-loop and out-of-loop modulation microwave.



Fig.49 Sage 6708-2 mechanical phase shifter

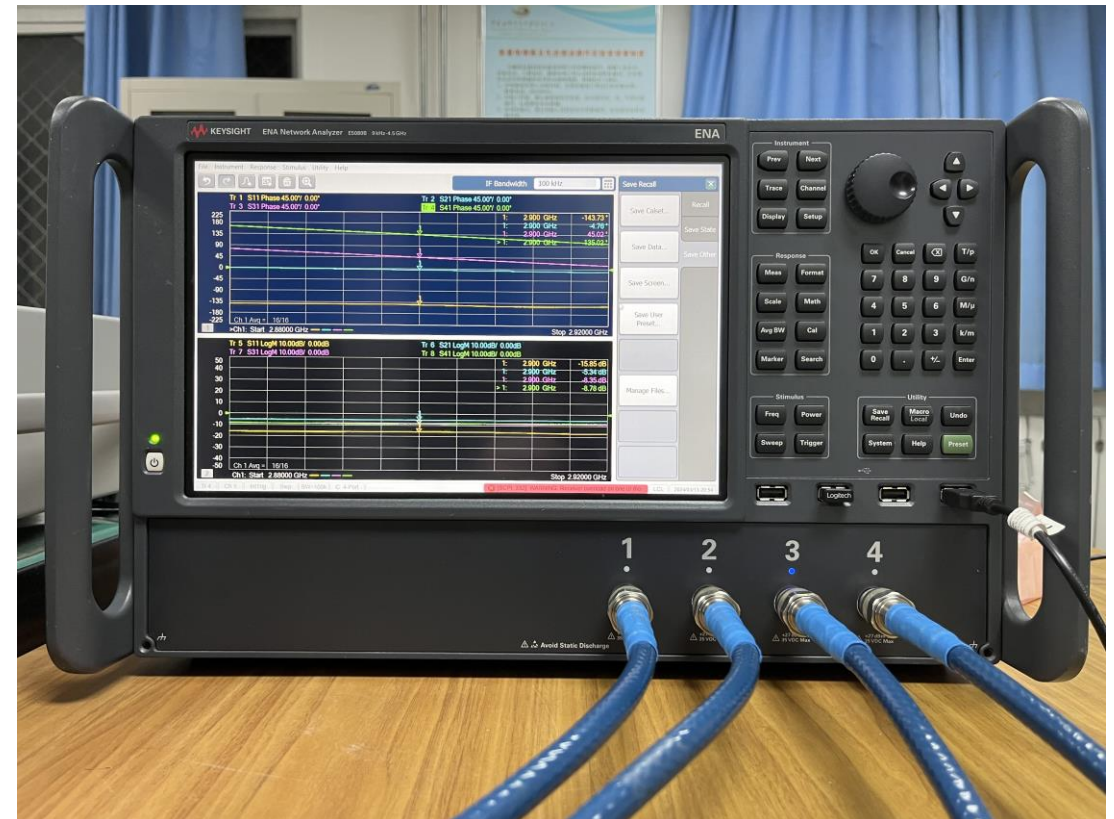


Fig.50 Keysight E5080B ENA Network Analyzer



Experimental Setup of Synchronization and Testing System

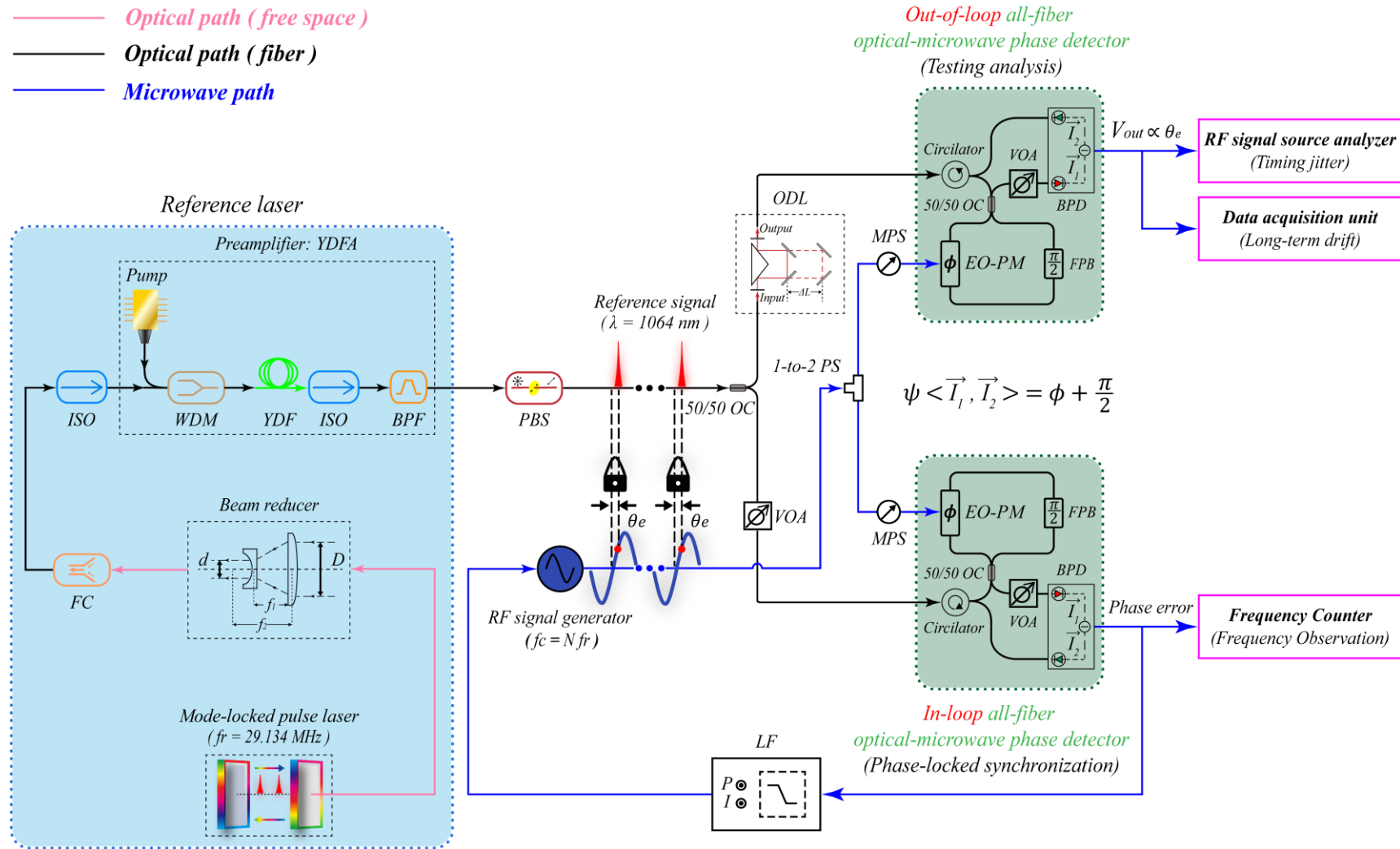


Fig.51 Experimental setup of laser-RF synchronization and testing system based on AFOM-PD

Experimental Results

- AFOM-PD phase detection sensitivity under 1.311030 GHz and 2.855132 GHz microwave modulation;
- Residual phase noise of the synchronized microwave and corresponding RMS integrated timing jitter (*1 Hz to 1 MHz*)
- Long-term RMS timing drift of the synchronized microwave over *6 h*.



AFOM-PD Phase Detection Sensitivity



Fig.52 The synchronized and testing system in operation.

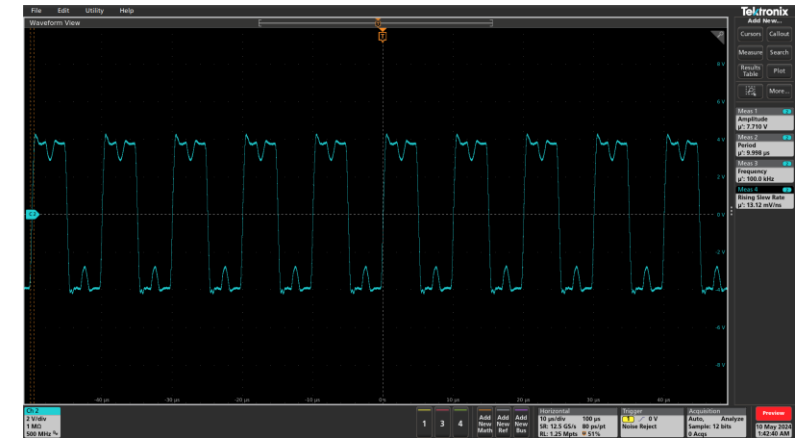


Fig.53 100 kHz error waveform under 1.311030 GHz microwave modulation



Fig.54 100 kHz error waveform under 2.85132 GHz microwave modulation



AFOM-PD Phase Detection Sensitivity

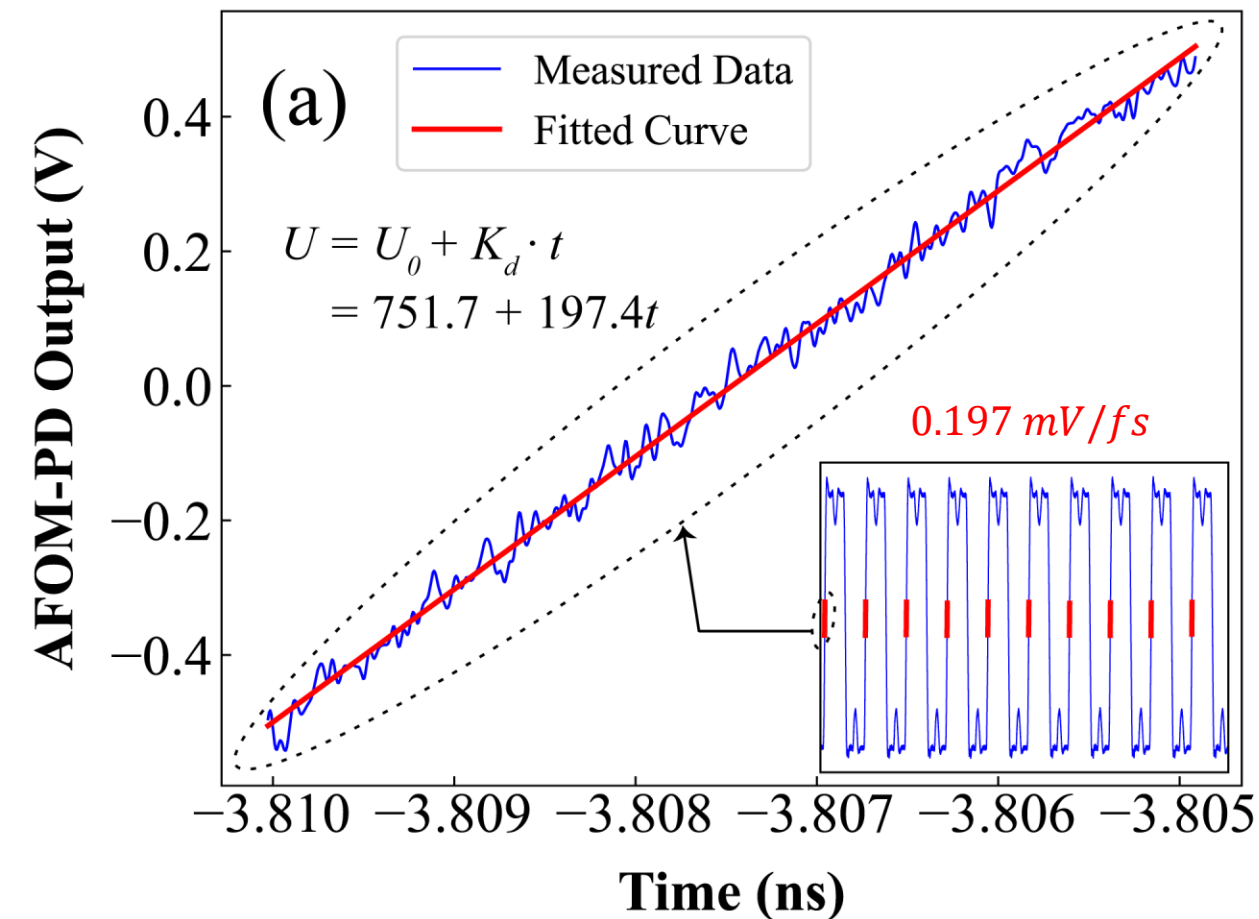


Fig.55 The error signal waveform and rising edge fitting curve under 1.311030 GHz microwave modulation

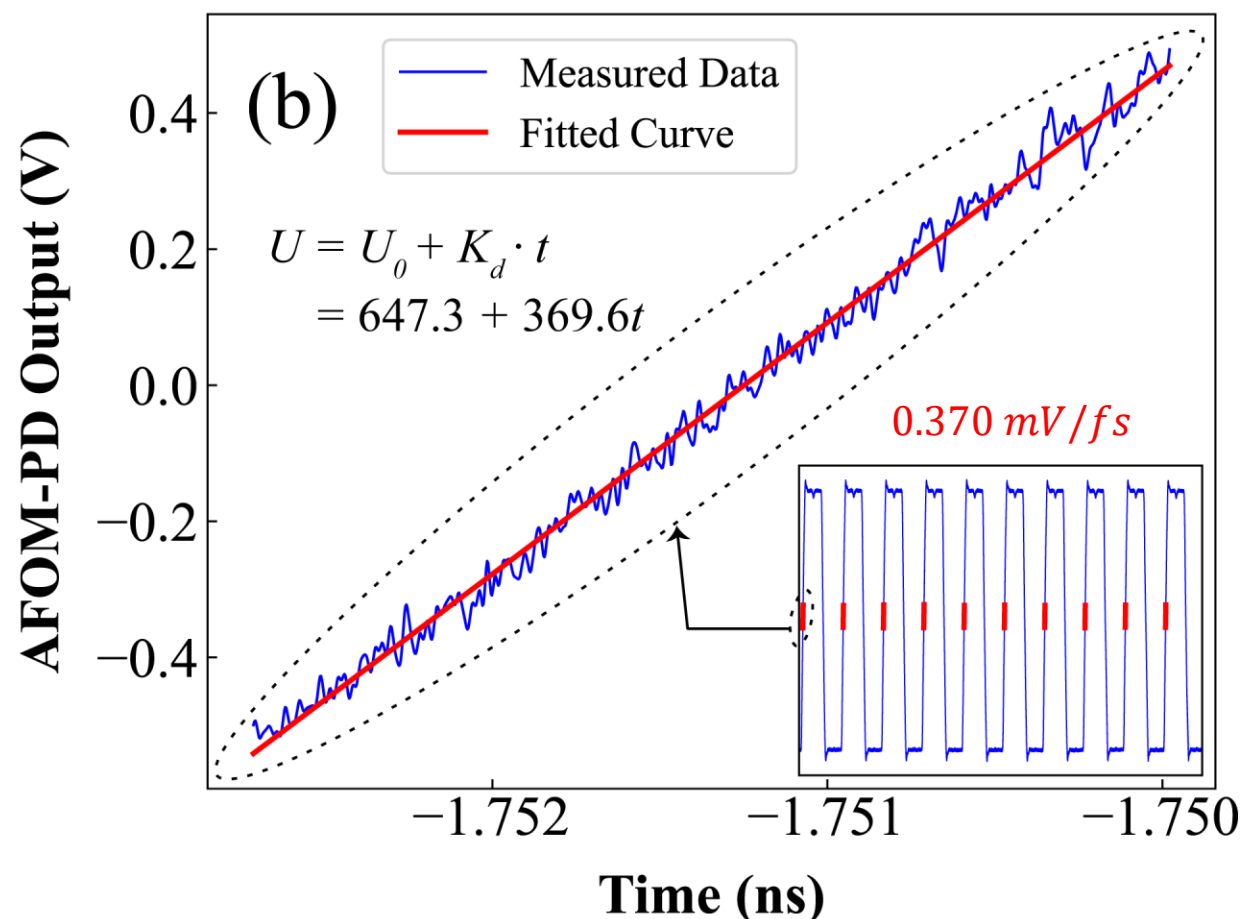


Fig.56 The error signal waveform and rising edge fitting curve under 2.855132 GHz microwave modulation



Residual Phase Noise and RMS Integrated Timing Jitter

- Single-side band power spectral density, $S_\phi(f)$
- Single-side band residual phase noise, $\mathcal{L}_\phi(f)$
- $S_\phi(f)$ and $\mathcal{L}_\phi(f)$:

$$\mathcal{L}_\phi(f) = 10 \log_{10} \left[\frac{S_\phi(f)}{2} \right]$$

- RMS integrated timing jitter:

$$\Delta t_{RMS} = \frac{1}{2\pi f_c} \sqrt{\int_{f_1}^{f_2} S_\phi(f) df}$$

Where $[f_1, f_2]$ is the integrated offset frequency range.

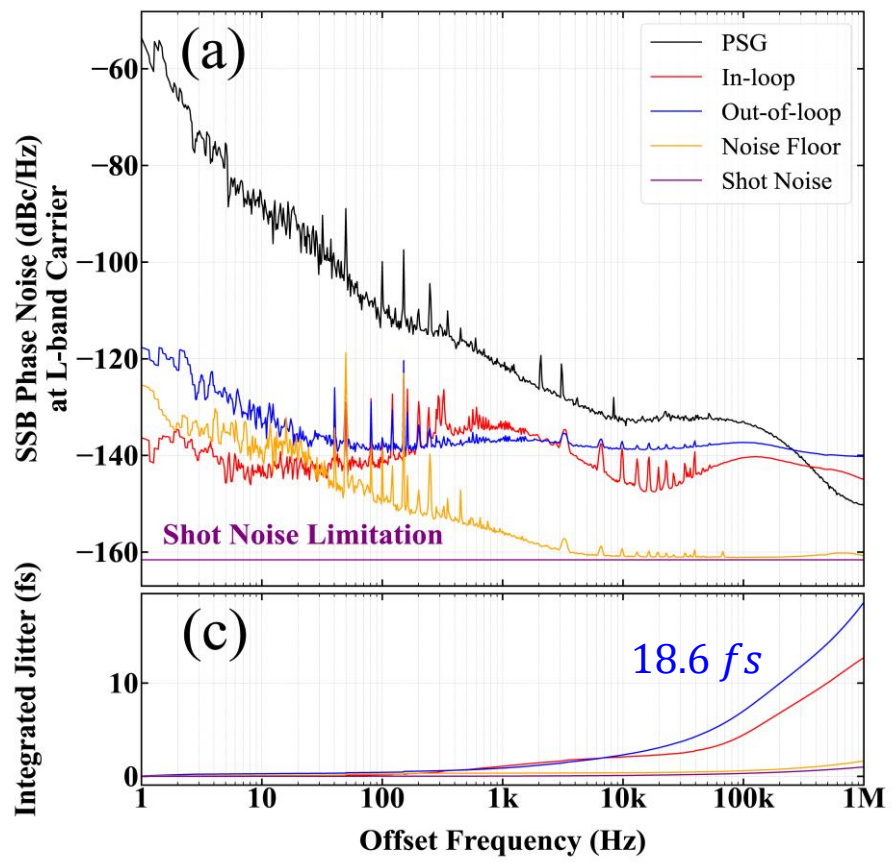


Fig.57 Residual phase noise of the synchronized 1.311030 GHz microwave (a) and RMS integrated timing jitter (c).

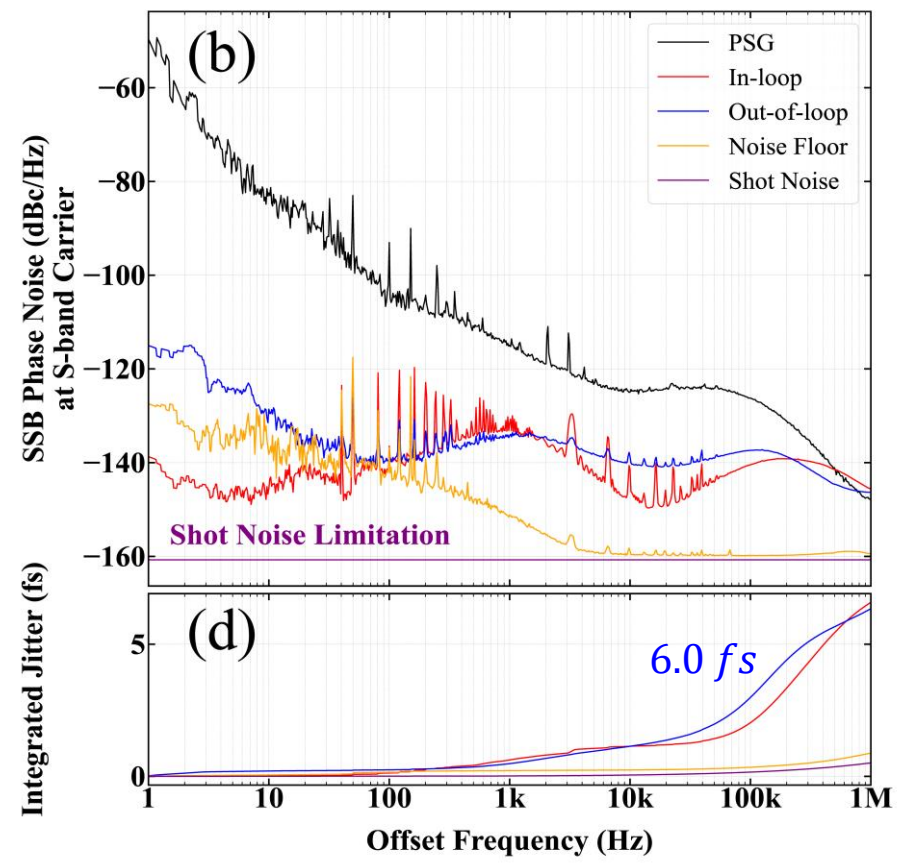


Fig.58 Residual phase noise of the synchronized 2.855132 GHz microwave (a) and RMS integrated timing jitter (c).



Long-term RMS Timing Drift

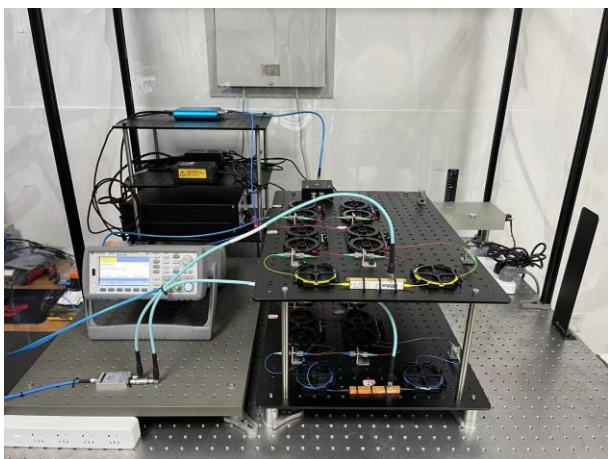


Fig.59 Long-term timing drift measurement



Fig.60 under temperature and humidity variations of 2 °C and 12.2%

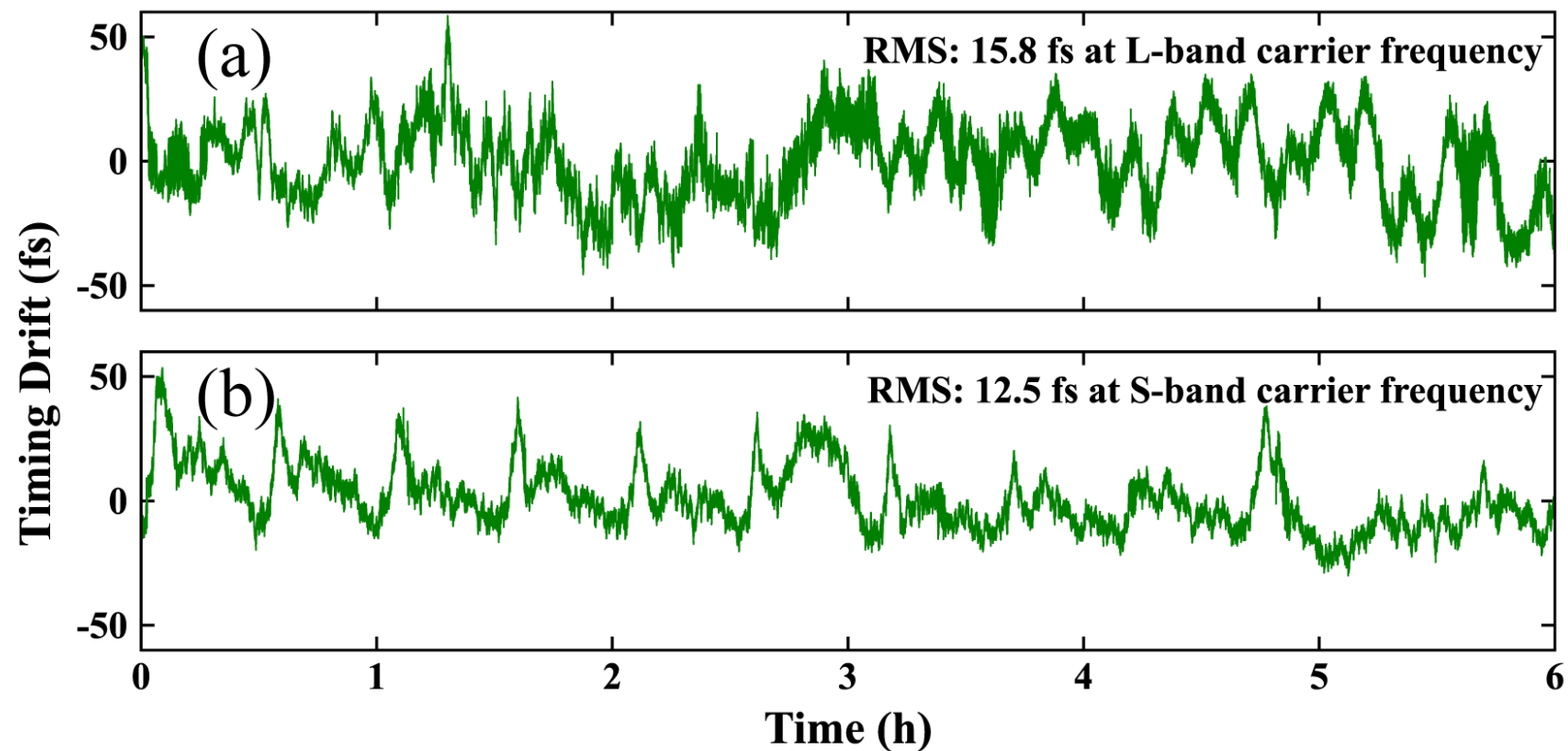


Fig.61 Long-term RMS timing drift of the synchronized microwave over 6 h at 1.311030 GHz (top) and 2.855132 GHz (bottom)

Future plans

- Some improvements, including the reference laser and the structure of the phase detector, have been implemented in the second synchronization system.
- The development of 2nd laser-RF synchronization system based on dual-balanced all-fiber optical-microwave phase detectors (DB-AFOMPDs) will complete performance testing in December 2024. Once engineering is finalized, it will be considered for use as a phase reference line for beam-driven plasma wakefield accelerators in IHEP.



Synchronization System Based On DB-AFOMPD

- The seed laser has been changed to a femtosecond fiber laser with 300-fs pulse width and 81.25 MHz repetition frequency.
- The improved laser-microwave synchronization system will achieve tunability of the reference laser wavelength within a certain range.
- Dual-balanced All-fiber Optical-microwave Phase Detector (DB-AFOM)
 - ❑ The optical path structure using a dual-balanced detection method
To further suppress the impact of laser RIN on the phase detector noise floor.
 - ❑ Temperature control based on semiconductor thermoelectric module
Precise temperature control (~ 0.01 °C) for sensitive optical and electronic devices.
- Completing performance testing in December 2024. This system will be considered for use in the **beam-driven plasma wakefield accelerators** (PWFA) of IHEP.

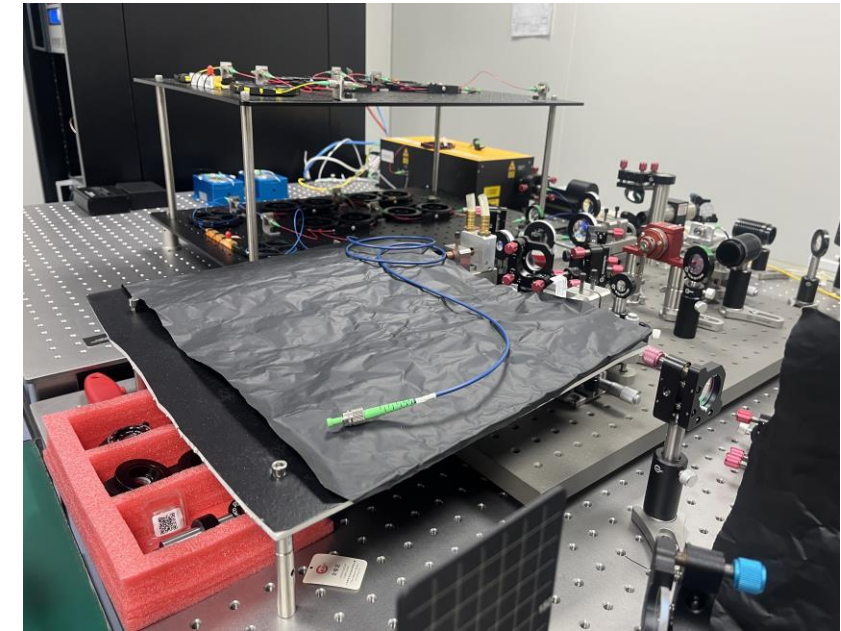


Fig.62 The unfinished DB-AFOMPDs



Laser-RF Synchronization System

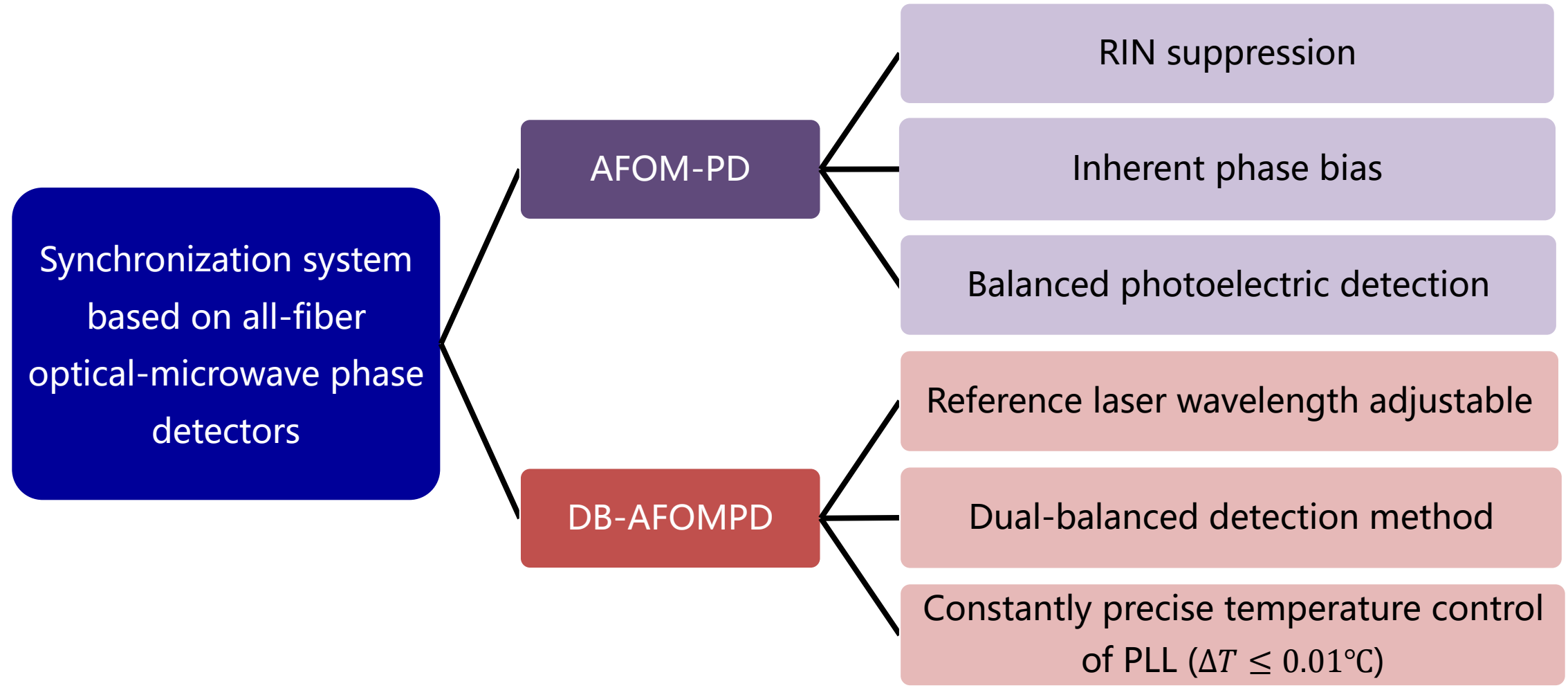


Fig.63 Synchronization systems and OMPDs



Conclusion

- A femtosecond-level synchronization system based on all-fiber optical-microwave phase detectors (AFOM-PDs) has been demonstrated.
 - ❑ The RMS integrated timing jitter out-of-loop for the synchronized **1.311030 GHz** microwave is **18.6 fs**, while the integrated timing jitter inside the loop is **12.7 fs**;
 - ❑ The RMS integrated timing jitter out-of-loop for the synchronized **2.855132 GHz** microwave is **6.0 fs**, while the integrated timing jitter inside the loop is **6.9 fs**;
- The long-term time drift over **6 h** for the synchronized **1.311030 GHz** and **2.855132 GHz** microwaves is **15.8 fs** and **12.5 fs**, respectively.
- The 2nd synchronization system based on dual-balanced all-fiber optical-microwave phase detectors (DB-AFOMPDS) will test by the end of this year.

Thank you!

Hao Zeng

Institute of High Energy Physics, Chinese Academy of Sciences

E-mail: zengh@ihep.ac.cn

Address: IHEP, No.19B Yuquanlu Road, Shijingshan District, Beijing, China.